



ORTHO-EQUILIBRIUM AND PARA-EQUILIBRIUM PHASE DIAGRAMS FOR INTERSTITIAL / SUBSTITUTIONAL IRON ALLOYS

Ernst Kozeschnik
Materials Center Leoben, Austria, and
Inst. for Materials Science, Welding and Forming
Graz University of Technology
Kopernikusgasse 24, A-8010 Graz, Austria

John M. Vitek
Oak Ridge National Laboratory
P.O. Box 2008
Oak Ridge, TN, 37831-6096, U.S.A

ABSTRACT: A mathematical model for the evaluation of compositionally constrained thermodynamic equilibrium has recently been implemented into the computer program MatCalc. This model is applied to the calculation of para-equilibrium phase diagrams for some ternary model iron alloy systems Fe-X-C, with X = Mn, Ni, Cr and Mo. The results are compared to the corresponding full equilibrium (ortho-equilibrium) phase diagrams and the impact of each element on the austenite / ferrite / carbide transformation in steels is analyzed. The para-equilibrium phase diagrams are considerably more simple than the potentially complex ortho-equilibrium phase diagrams, showing cementite formation as the only stable carbide under para-equilibrium conditions. The driving forces for precipitation of cementite and the complex chromium carbides in the Fe-Cr-C system are evaluated as a function of the precipitate composition. The evaluation of the driving forces under para-equilibrium conditions predicts carbide precipitation behavior that agrees with experimental findings.

Introduction

Equilibrium phase diagrams are a basic and useful tool for the metallurgist when analyzing phase transformations in multi-phase, multi-component alloys. These diagrams can give an idea of which phase transformations might occur when, for instance, quenching an alloy from an austenitization temperature to a certain transformation temperature. However, in many multicomponent systems, it is observed that the final full equilibrium state is approached in several consecutive, clearly separable steps. For instance, it is well known that the austenite to ferrite reaction in steels can occur by a rapid carbon-diffusion controlled process and a subsequent slow, substitutional-diffusion controlled reaction step. Whereas the carbon-controlled reaction approaches the para-equilibrium [1] state and is usually completed within seconds or minutes, the sluggish substitutional-diffusion reaction would take months or even years to finish. For that reason, full equilibrium (ortho-equilibrium) phase diagrams are sometimes of limited practical value for application to phase transformations in interstitial / substitutional alloys and para-equilibrium phase diagrams should be utilized instead.

The aim of the present work is to apply a recently developed model, which is suitable for the evaluation of constrained equilibria, to the evaluation of para-equilibrium phase diagrams for some ternary and higher-order interstitial / substitutional model systems. After comparing the ortho-equilibrium and para-equilibrium phase diagrams, the model is used to calculate the driving force for precipitation of cementite, $M_{23}C_6$ and M_7C_3 particles in a 2.8 % Cr steel. The necessary thermodynamic information is taken from the SGTE-solution database [2].

Received 18 January 2000

The constrained thermodynamic equilibrium model

The mathematical formalism of the compositionally constrained equilibrium model is based on the Gibbs free energy minimum principle

$$G_m = \sum_i f^i \cdot G_m^i = \text{Minimum} \quad (1)$$

where G_m is the molar Gibbs free energy of the system, G_m^i is the molar Gibbs free energy of phase i and f^i is the corresponding phase fraction variable. The Gibbs free energy of each phase is expressed in terms of the sublattice model proposed by Hillert and Staffansson [3] and is thus a function of temperature T , pressure P , the phase composition variables y and a term contributing to magnetic ordering effects. When minimizing the Gibbs free energy of the system (equation 1), the formal constraints of the sublattice model as well as the compositional (para-equilibrium) constraints are implemented by the Lagrange multiplier technique. Further details are given in reference [4].

Ortho-equilibrium and para-equilibrium phase diagrams

In order to demonstrate the impact of para-equilibrium constraints on equilibrium phase diagrams, various ortho-equilibrium and metastable para-equilibrium Fe-C-X phase diagrams have been calculated using the previously described compositionally constrained equilibrium model. The symbol X represents the elements Mn, Ni, Cr and Mo. The results are presented in figures 1 to 4. Looking at these figures, it is immediately observed that the imposed para-equilibrium constraints reduce the ternary systems to simple quasi-binaries. The compositional constraint on the Fe to X ratio in all phases, including the carbide precipitates, defines a new compound consisting of Fe and X atoms with constant ratio. As the Fe/X ratio is fixed, the para-equilibrium constraints reduce the degrees of freedom of the systems by one and, according to the Gibbs phase rule, there can be no three-phase fields in the para-equilibrium case.

It is very interesting to analyze the impact of each of the alloying components on the stable and metastable equilibrium phase diagrams. From figure 1, it is observed that para-equilibrium constraints for manganese lower the ferrite transformation start temperature (line between regions 1 and 2) by approximately 35 °C. On the other hand, at very low carbon contents, the para-equilibrium eutectoid temperature can be significantly higher than the corresponding temperature under full equilibrium conditions. It has recently been concluded [5] that, on quenching, this fact allows for the formation of metastable para-equilibrium cementite that is not stable under full equilibrium conditions. Experimental evidence for the existence of paraequilibrium cementite is described in e.g. refs. [6,7] for the tempering of martensite. Furthermore, at very low carbon content, austenite could transform into 100 percent ferrite according to the para-equilibrium phase diagram, whereas under ortho-equilibrium conditions the system would still be in the austenite / ferrite two-phase field. Consequently, austenite could completely dissolve by a rapid reaction and subsequently re-precipitate when approaching the full equilibrium state. For a further discussion, the reader is referred to reference [5].

Nickel is a very effective austenite stabilizer. Like manganese, in ortho-equilibrium, nickel opens a wide austenite / ferrite / cementite three-phase field (see figure 2). In para-equilibrium, this region is reduced to a quasi-eutectoid temperature at approximately 675 °C. The Fe-Ni-C para-equilibrium phase diagram is nearly identical to the Fe-Mn-C para-equilibrium diagram, with only small shifts in the transformation temperatures.

Chromium is a typical ferrite stabilizer and a strong carbide former. In addition to the cementite phase, three complex chromium carbides (M_2C_6 , M_7C_3 and M_3C_2) can occur in the Fe-Cr-C system. The ortho-equilibrium and para-equilibrium phase diagrams are shown in figure 3. Due to the existence of the additional carbides, the ortho-equilibrium phase diagram is more complex than the previously presented diagrams. However, if para-equilibrium constraints are imposed on the simulations, the diagram resembles the para-equilibrium phase diagrams of the other ternary systems. Under para-equilibrium transformation conditions, the complex chromium carbides become unstable and only the cementite phase can form (meta)stable precipitates. This finding is in accordance with the experimental experience that the formation of complex carbides involves the long-range diffusion of substitutional alloying components and therefore needs longer tempering times [8]. This issue will be discussed in more detail in the subsequent section.

The Fe-Mo-C phase diagram (figure 4) is even more complex than the Fe-Cr-C phase diagram. Various carbide phases can form under full equilibrium conditions, i.e. Mo_2C , Mo_6C , the 'Ksi-carbide' and the 'MC_SHP-carbide'. However, similar to the Fe-Cr-C system, the para-equilibrium phase diagram shows only the austenite, ferrite and

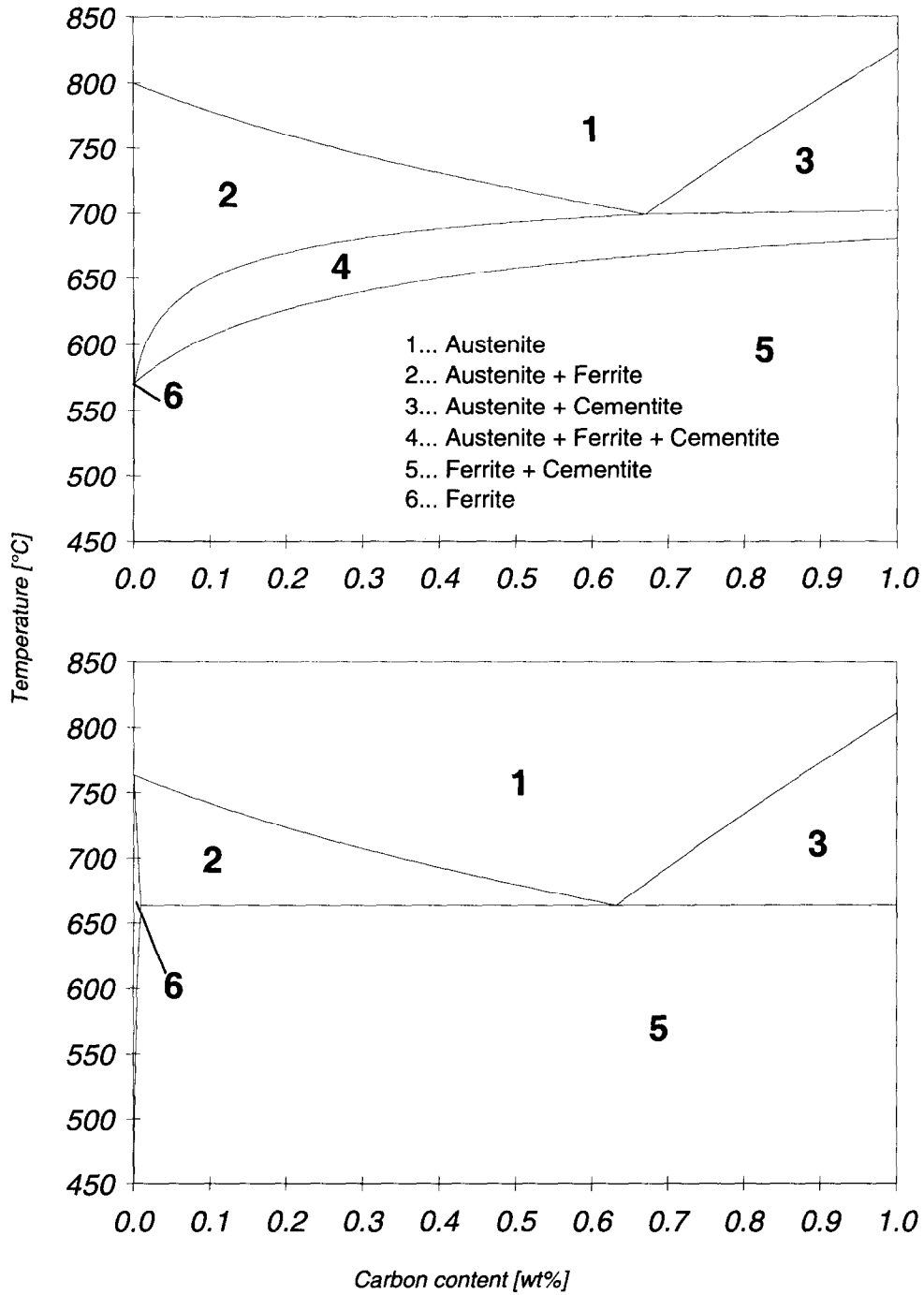


FIG. 1

Calculated ortho-equilibrium (upper) and para-equilibrium (lower) phase diagrams of Fe-C-3 wt% Mn.

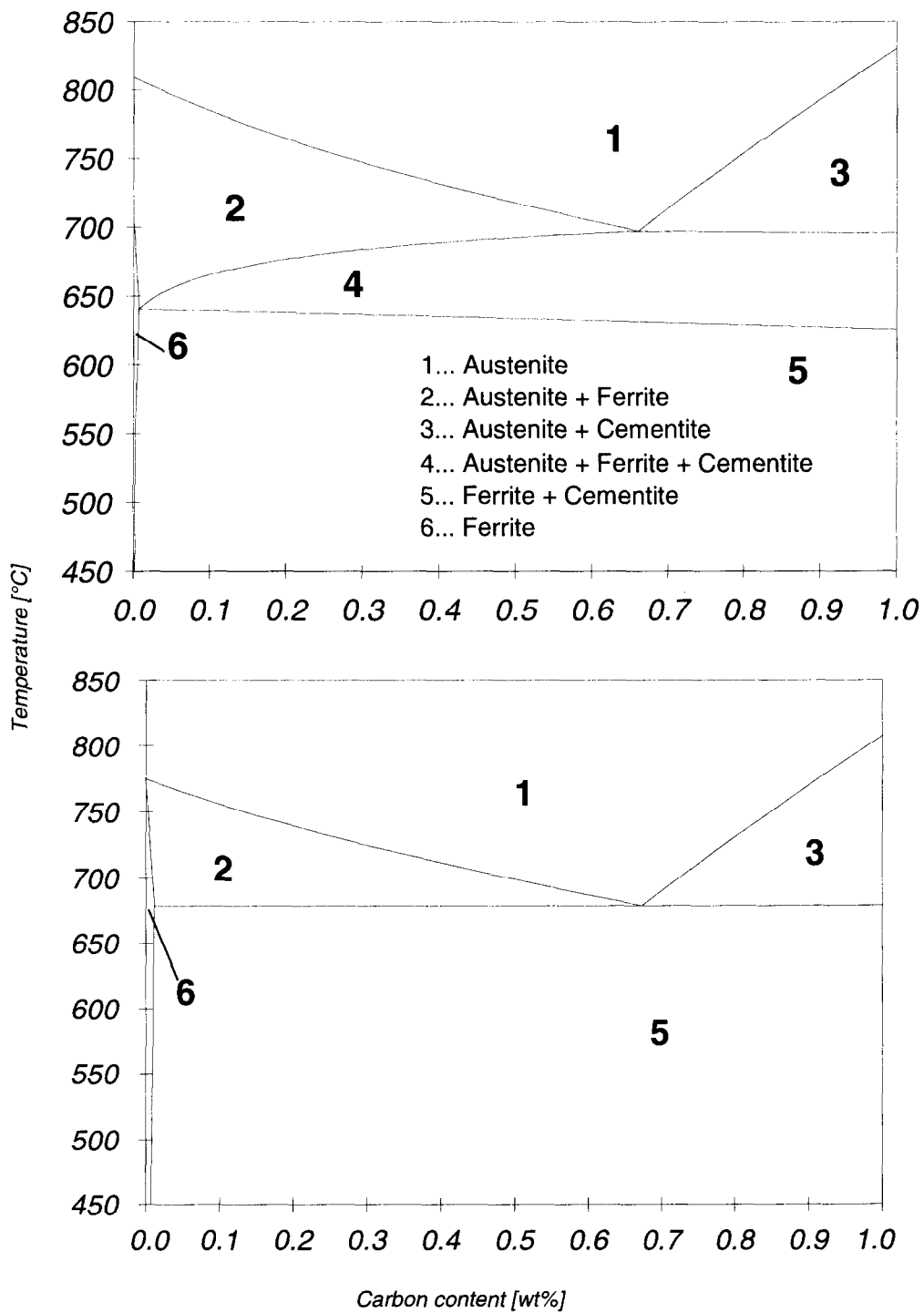


FIG. 2

Calculated ortho-equilibrium (upper) and para-equilibrium (lower) phase diagrams of Fe-C-3 wt% Ni.

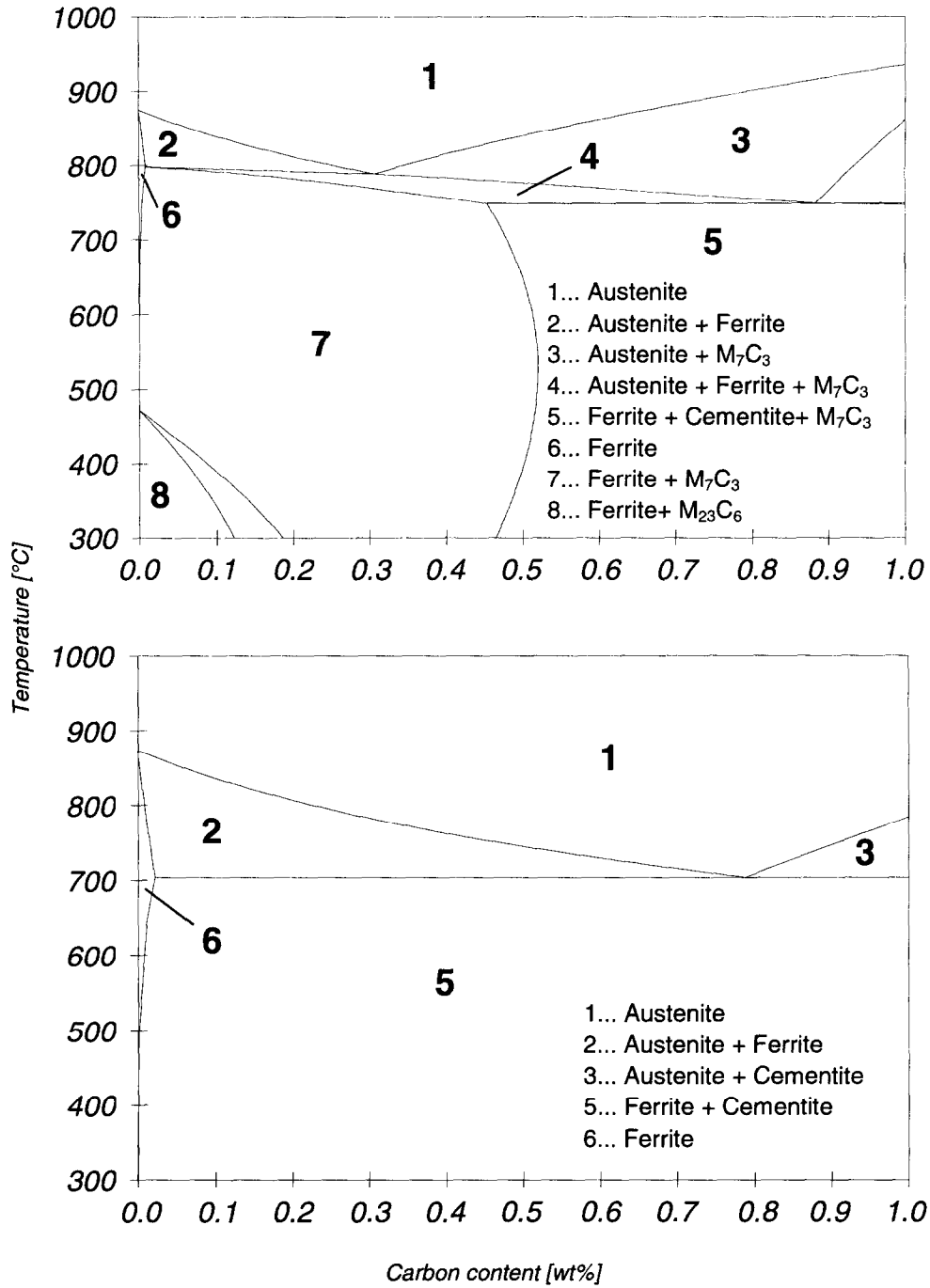


FIG. 3

Calculated ortho-equilibrium (upper) and para-equilibrium (lower) phase diagrams of Fe-C-2.8 wt% Cr.

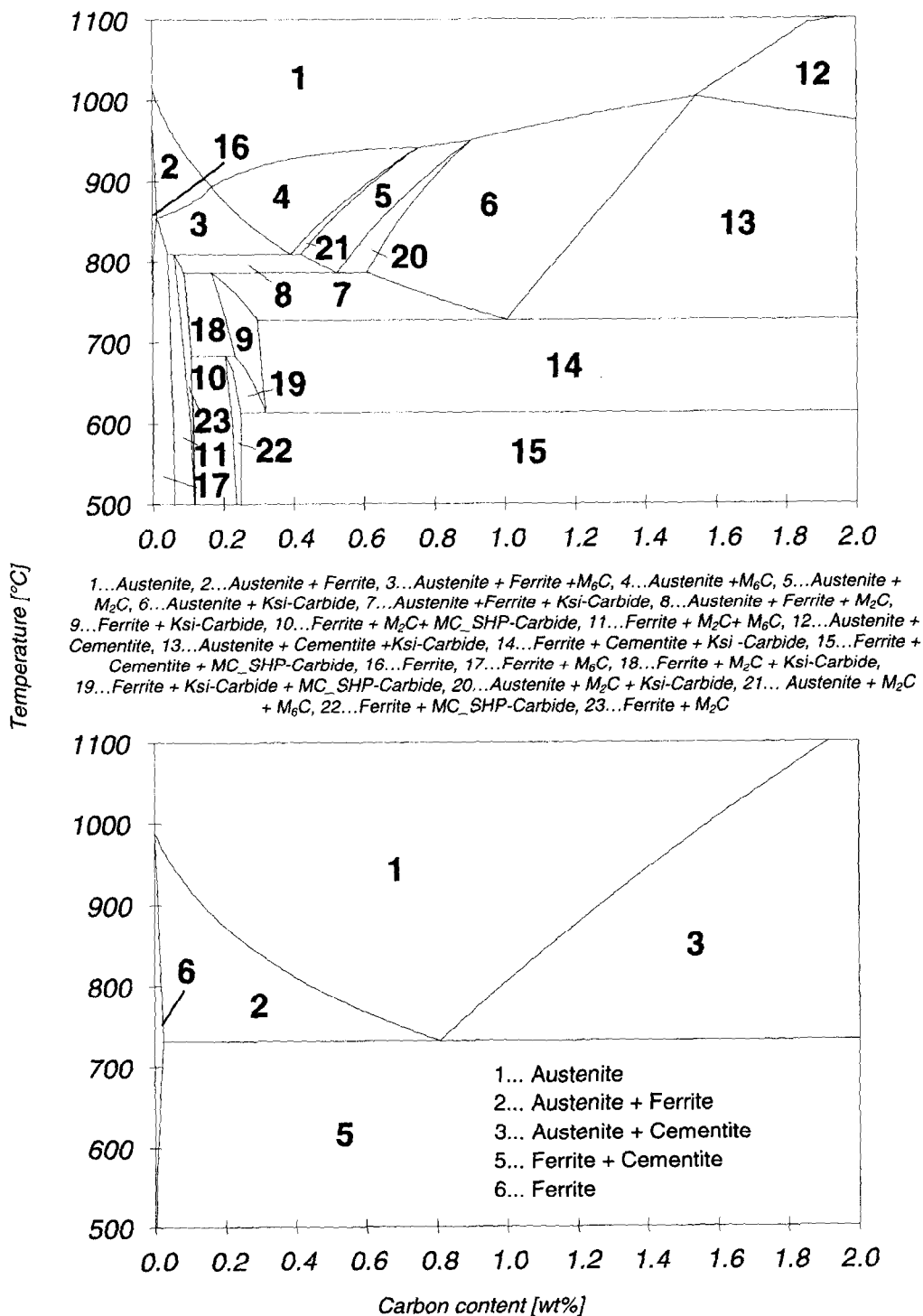


FIG. 4

Calculated ortho-equilibrium (upper) and para-equilibrium (lower) phase diagrams of Fe-C-2 wt% Mo.

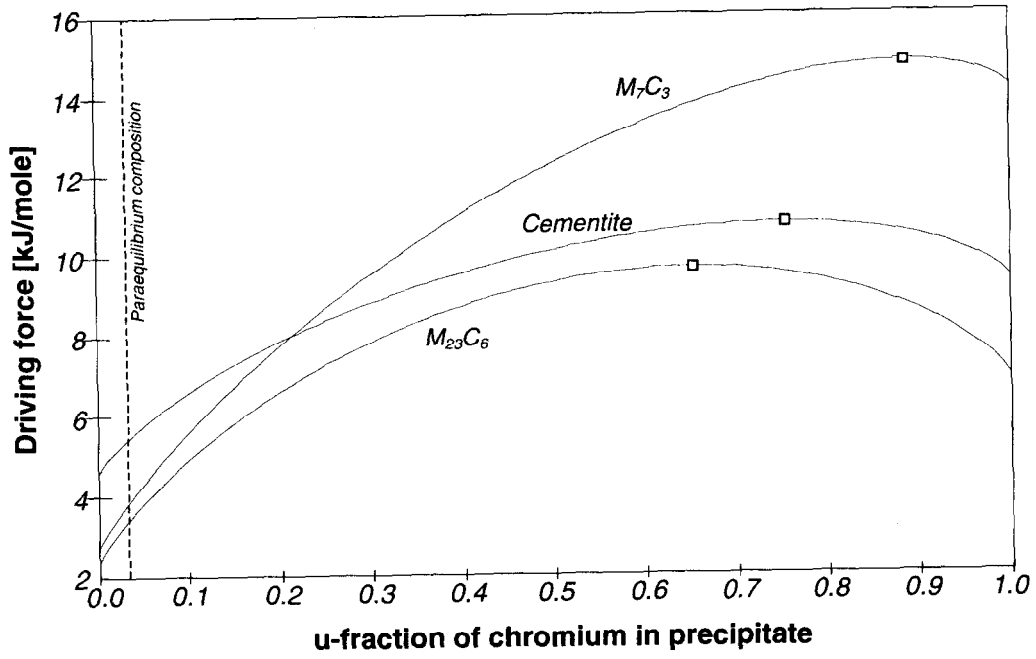


FIG. 5

Calculated chemical driving force for precipitation of carbides in of Fe - 0.15 wt% C - 2.8 wt% Cr at 600 °C.
 Square symbols represent the ortho-equilibrium compositions.

cementite phase. All complex carbides are unstable under para-equilibrium conditions. Again, this result is in accordance with the experimental evidence [9].

Chemical driving force for second-phase precipitation in Fe - 0.15 wt% C - 2.8 wt% Cr

The precipitation of iron/chromium carbides (cementite, $M_{23}C_6$ and M_7C_3) is accompanied by long-range diffusion of carbon and chromium atoms. Since the diffusion coefficient of chromium is several orders of magnitude lower than the diffusion coefficient of carbon, nucleation and growth of the particles initially occur in the para-equilibrium regime. Figure 5 presents the calculated driving forces for precipitation of the three carbides as a function of the carbide composition at 600 °C. The μ -fraction variable printed on the X-axis denotes the fraction of chromium on the substitutional sublattice only. The chemical driving force ΔG_i of phase i is calculated with

$$\Delta G_i = \sum_k X_k^i \mu_k - G_i^m \quad (2)$$

where X_k^i is the mole fraction of component k , μ_k is the chemical potential and G_i^m is the molar Gibbs free energy of the carbide.

Figure 5 demonstrates that, at low chromium content in the precipitates, cementite has the highest driving force. With increasing chromium content, the complex M_7C_3 has the highest driving force. Again, this result is in accordance with the experimental evidence [10] that in quenched and tempered martensite the first precipitate to occur is usually the cementite whereas the complex M_7C_3 and $M_{23}C_6$ precipitate only after prolonged annealing.

Conclusion

The calculated para-equilibrium phase diagrams correctly reflect the effects of Mn, Ni, Cr and Mo on the austenite / ferrite / carbide phase transformation. The predicted phase constitution after the rapid carbon-diffusion controlled austenite decomposition reaction is in general agreement with the experimentally observed metastable microstructure of similar steels. The computed chemical driving forces for precipitation support the observed precipitation sequence in tempered martensite.

Acknowledgement: The work of E. Kozeschnik was sponsored by the *Materials Center Leoben*, Austria and carried out at the Institute for Materials Science, Welding and Forming of the Graz University of Technology, Austria. Research by J. M. Vitek was sponsored by the Division of Materials Sciences and Engineering, U.S. Department of Energy, under contract DE-AC05-00OR22725 with UT-Battelle.

References:

- 1 A. Hultgren: *Trans. ASM*, **39**, 915 (1947).
- 2 SGTE solution database (1992), Editor: B. Sundman, Division of Computational Thermodynamics, Royal Institute of Technology, Stockholm, Sweden.
- 3 M. Hillert, L.-I. Staffansson: *Acta Chem. Scand.*, **24**, 3618 (1970).
- 4 E. Kozeschnik, *CALPHAD*, (2000), in print.
- 5 E. Kozeschnik, *J. Phase Equil.*, **21** (4), 336 (2000).
- 6 R.C. Thomson, M.K. Miller, *Acta Mater.*, **46** (6), 2203 (1998).
- 7 S. S. Babu, K. Hono, T. Sakurai, *Metall. Mater. Trans. A*, **25A**, 499 (1994).
- 8 A. Inoue, T. Masumoto, *Metall. Trans. A*, **11A**, 739 (1980).
- 9 D.V. Shtansky, G. Inden, *Acta Mater.*, **45** (7), 2861 (1997).
- 10 R.G. Baker, J. Nutting, *J. Iron Steel Inst.*, **192**, 257 (1959).